Durable Chiral Sensor Based on Quartz Crystal Microbalance Using Self-Assembled Monolayer of Permethylated *β*-Cyclodextrin

Siu-Choon Ng[*], *Tong Sun, Hardy S. O. Chan**

Department of Chemistry, National University of Singapore, Lower Kent Ridge Road, Singapore 117543
Email: chmngsc@leonis.nus.edu.sg; chmcsoh@nus.edu.sg

Summary: A novel chiral sensor based on quartz crystal microbalance (QCM) with a self-assembled monolayer of permethylated β-cyclodextrin as the enantioselective coating has been derived which exhibit improved enantioselectivity and excellent long-term environmental stability when used in gas phase sensing.

Introduction

The detection of individual enantiomer remains a challenging task in analytical chemistry, since enantiomers exhibit their individualities only in a chiral environment. Although chromatographic methods like HPLC, GC, CE, using chiral stationary phases (CSPs), are efficient for enantioseparations, they are time-consuming and not readily adaptable for real time determination of enantiomers.[1] Meanwhile, gravimetric sensors like quartz crystal microbalance (QCM) and surface acoustic wave (SAW) devices have shown promise as rapid, sensitive and portable transducer elements for chemical sensing.[2] Several appeared recently describing the application of QCM for chiral sensing in gas phase. Ide et al.[3] reported on the use of quartz-resonator gas sensor coated with cyclodextrins films to discriminate optical isomers of rose oxide and citronellal, although the results were questioned by others.[4] Thereafter, Bodenhöfer et al.[4,5] carried out detailed studies of gas phase discrimination of enantiomers on QCM spin-coated with Chirasil-Val film. These studies show that the design of chiral sensor based on QCM transducer with an appropriate chiral coating is feasible in the gas phase. However, in these works, the chiral coatings were deposited using physical method, which has the drawback of poor durability that could impair the discriminative efficiency of the chiral sensor. Unlike GC or HPLC, which has thousands of "plates" in the column on which adsorption/desorption processes take place, QCM chiral sensor has only one

"theoretical plate" available for interactions with guest molecules.[4] Consequently, the surface arrangement of the enantioselective elements on quartz surface can be crucial in achieving premium chiral discrimination performance.[6] Spin-coating and airbrushing methods are unlikely to afford an ordered surface of functional coating, thus the effective chiral host-guest interactions might be impaired. Moreover, these coating methods could also result in the easy loss of functional materials over time, as we have noticed.[7] It was envisaged that a chemically bonded enantioselective layer would overcome this disadvantage. However, to the best of our knowledge, there has been no reported work on the design of QCM chiral sensor coated with self-assembled functionalized β-cyclodextrins (βCD).

In the present work, we undertook a systematic approach to demonstrate this design of QCM chiral sensor based on self-assembled permethylated βCD for gas phase chiral discrimination with enhanced chiral discriminatory performance and improved durability of functional coatings. Permethylated βCD molecule was immobilized on Au electrodes of a 10 MHz AT-cut quartz plate through single thiol linkers, $NH_2(CH_2)_nSH$, of different lengths, n=2, 6, 11, respectively. The surface concentration of resulted monolayers was calculated. From the real-time responses of the QCM upon exposure to enantiomeric analytes, the chiral discriminatory ability of the different permethylated βCD monolayers was compared.

Experimental

The mercaptyl functionalizaed β-cyclodextrins were synthesized in accordance to Scheme 1 using an extended application of the Staudinger reaction.[8]

Reagents and Conditions: (i) p-TsCl / Pyridine (dry); (ii) NaN$_3$ (aq.) / Δ; (iii) MeI / NaH / DMF (dry); (iv) NH$_2$(CH$_2$)$_n$SH / CO$_2$ / Ph$_3$P / THF (dry); (v) absolute ethanol / 24 hrs.

In this scheme, $NH_2(CH_2)_nSH$ with n=2, 6, 11, respectively, was attached to the 6^A position of $(6^A$-azido-6^A-deoxy)heptakis(2,3-di-O-methyl)- 6^B, 6^C, 6^D, 6^E, $6^F,6^G$-hexa-O-methyl-β-cyclodextrin, respectively. The products are denoted as **CD1**, **CD2**, and **CD3**, accordingly. The structures and purities of the β-CD derivatives were confirmed by NMR spectroscopy (Bruker DPX 300 spectrometer), Electron-spray-ion mass spectroscopy (ESI-MS) (Finnigan TSQ7000 mass spectrometer), FTIR spectroscopy (Perkin Elmer 1600 spectrometer), and Elemental analysis (Perkin Elmer 240C elemental analyzer. C, H, N, and S, within ±0.5% errors). Detailed structural data are given in the last part of this paper. Using established self-assembled monolayer (SAM) procedure compounds **CD1-3** were immobilized onto the surface of Au electrodes of QCM.[9]

Time-of-flight secondary ion mass spectra (TOF-SIMS) of the monolayers were obtained with an ION-TOF GmbH instrument using a pulsed primary beam of Ar ions (10 KeV) under static conditions. Spot size is 10×10 μm^2.

The topographic images of the immobilized β-CD monolayers were obtained with a Nanoscope II (Digital Instruments, Santa Barbara, CA) Atomic Force Microscopy (AFM) in non-contact mode, 1 $\mu m \times 1$ μm scanning area.

The QCM employed is a commercially available 10 MHz, AT-cut quartz, purchased from International Crystal Manufacturer, Inc., Oklahoma City, USA. The quartz crystal plate was deposited with Au electrodes (diameter 0.201") on both sides (area 0.20 cm^2). The QCMs were cleaned with "*pirhana*" solution of 30% H_2O_2/70% conc. H_2SO_4 (v/v) at 70°C just prior to monolayer deposition (**Caution:** *pirhanan* solution reacts violently with organic compounds and must be used with extreme caution!). For TOF-SIMS and AFM experiments, commercial Au mirrors (Bio-Rad, Inc.) were used for monolayer deposition. After rinsing with copious Milli-Q water, the QCMs/Au mirrors were immersed into 10^{-3} M ethanol solution of **CD1-3** for 24 h. After the treatment with copious ethanol and Milli-Q water, the QCMs/Au mirrors were dried in N_2 stream until the frequency shift of the quartz plate remained constant, indicating the complete removal of physisorbed small molecules.

The gas phase measuring system used was similar in design to that in ref. 10. It includes a microscale vaporizer to allow for the evaporation of minute amounts of enantiomer samples and a thermostated flow-through measuring cell housing the QCM devices. Predried N_2 was used as carrier gas and controlled by an Alicat mass flow meter. The temperature of the vaporizer was maintained at 35 ± 0.1 °C with the measuring cell at 25 ± 0.1 °C. The volume of

the thermostated measuring cell (66.0 cm^3) can ensure the temperature of arrival N$_2$ gas stream on the surface of QCM to be 25.1±0.1 °C, no condensation of sample analytes was observed during the measurements. A Lab Crystal Oscillator of ICM Co. was used to generate the signal, and a TF830 universal counter to measure the frequency shifts. All data were record by an online PC.

Results and Discussion

CD1-3 Monolayers

The successful self-assembly of derived βCD molecules on Au surface was confirmed using TOF-SIMS. Figure 1 displays a typical spectrum of **CD3**/Au under 10 KeV Ar ionization. The
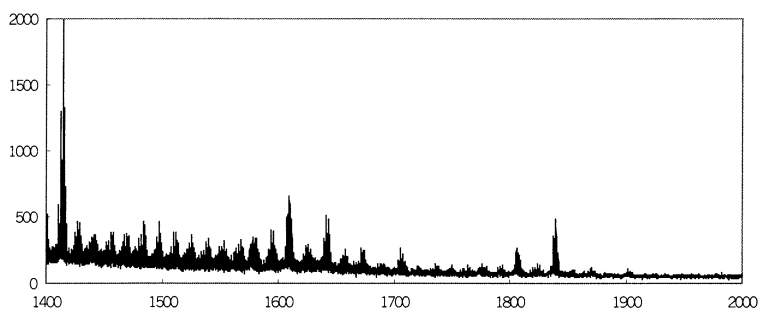
Figure 1. Positive TOF-SIMS spectrum of **CD3** monolayer on Au mirror.

presence of peaks at 1807 [M+Au-S]$^+$ and 1839 [M+Au]$^+$ (where M is the molecular mass of permethylated β-CD with a thiol linker, e.g. M_{CD3} =1643.7 g/mol) corroborates the successful confinement of **CD3** molecules on the Au surface.[11] Further evidence confirming the formation of **CD1-3** monolayer on Au surface was illustrated in Figure 2. As can be seen, there is no presence of particles at the height of 12nm on the surface of commercial bare gold (Figure 2a). After being immobilized with **CD1**, the surface looks rougher (Figure 2b). Typical particles with the diameter of 10-50nm are well observed at the height of 12-15nm.

The surface coverage of the monolayers can be directly calculated from the decrease of the resonant frequency (Δf) of quartz plate using the equation derived by Sauerbrey.[12] For AT-cut 10MHz quartz crystal, the mass-frequency response can be expressed as:

$$\Delta f = (-2.26 \times 10^{-6}) f_0^2 (\Delta m / A) \qquad (1)$$

where f_0 is the fundamental frequency of the quartz resonator (Hz), and A the surface area of

the resonator Au electrode (0.20 cm^2). Accordingly the mean surface concentrations of the three permethylated βCD derivatives were calculated to be 6.20 × 10^{-11}, 7.08 × 10^{-11} and 8.98 × 10^{-11} mol cm^{-2}, for **CD**1, **CD**2 and **CD**3, respectively. These data are consistent with a surface concentration approximating to the hexagonal closed packing model,[9b] where the CD torus lies parallel to the surface. Amongst the three monolayers, **CD**3 which has the longest linker appears to be more closely packed.
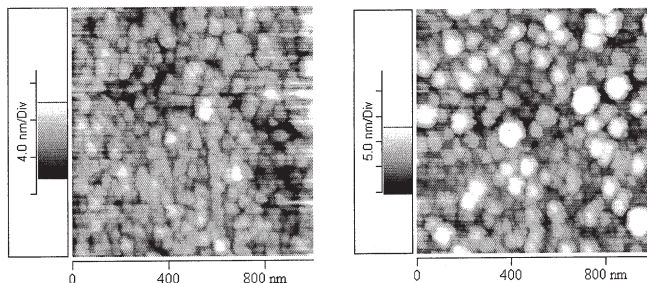
Figure 2. Topographic images of (a) bare Au surface; (b) **CD1** on Au surface.

Chiral Discrimination at Monolayers

Five pairs of pure enantiomers with different functional groups and various molecular size were selected to evaluate the enantiomeric discriminatory ability of the three derived sensors in gas phase. The frequency change of three QCM sensors (Δf) versus time plot are shown in Figure 3 with respect to the chiral analyte gas composition (R- and S-enantiomer). The overlay of the respective sensor signals affords better comparison between two enantiomeric forms. Meanwhile the repeatability of the sensor response is also depicted in Figure 4. As can be seen, the QCM sensor performances towards both forms of the chiral analyte are similar but differ in the extent in frequency reduction indicating the preferential binding presented by the permethylated βCD monolayers between R- and S-enantiomers, which affords the differences in the inclusion complexation amount (Δf) of the respective analytes on the monolayer. As being summarized in Table 1, the R-enantiomer of all five pairs of analytes invariably affords larger Δf than does the S-form indicating the higher binding affinity depicted by the permethylated βCD monolayers towards the R-enantiomer irrespective to the probably varied surface monolayer structure caused by the different length of thiol linkers.[13]

The chiral discriminatory factor, $\alpha_{R/S}$, of the three QCM sensors was calculated from the

equation: $\alpha_{R/S} = \dfrac{\Delta f_R}{\Delta f_S}$,[4] and listed in Table 1 along with the sensor recovery time, t. The chiral

discriminatory performances of our three sensors appear to fall into two categories: for
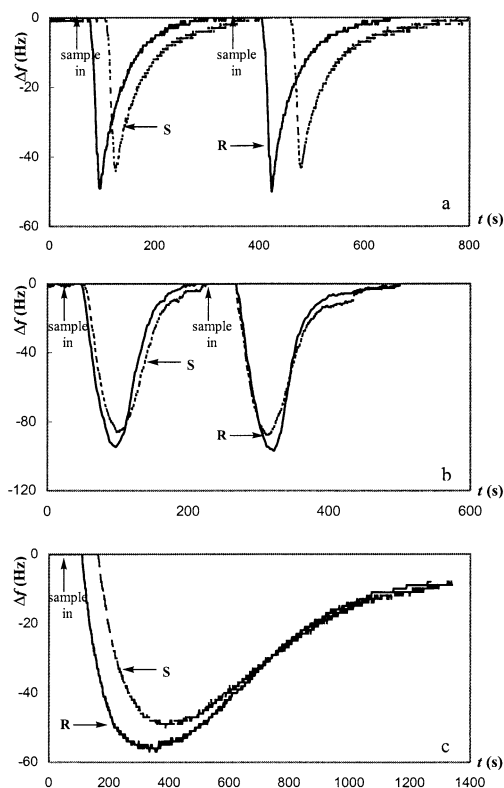

Figure 3. Typical time course of frequency change of three QCM sensors towards different chiral analytes. a) **CD1** vs methyl lactate (2.0 µl); b) **CD2** vs 2-octanol (0.5 µl); c) **CD3** vs carvone (1.0 µl)

analytes such as 2-butanol, methyl lactate, and ethyl lactate, which has relative small

molecular size, the $\alpha_{R/S}$ increases from **CD1** to **CD3,** corresponding to the enhanced inclusion

complexation of the guest molecules (Δf) on the monolayer from **CD1** to **CD3**. This can be

attributed to the increased surface concentration of immobilized βCD molecules on Au. On

the other hand, for 2-octanol and carvone, which has relatively large molecular size or rigid

structure, the inclusion complexation of both guest molecules decreases from **CD1** to **CD3**,

supported by the low $\alpha_{R/S}$ value of **CD3**. This phenomenon could be explained by the

formation of a quasi-two-layer structure in **CD3** monolayer,[14] which renders **CD3** monolayer less accessible interaction sites for larger guest molecules in the monolayer structure.
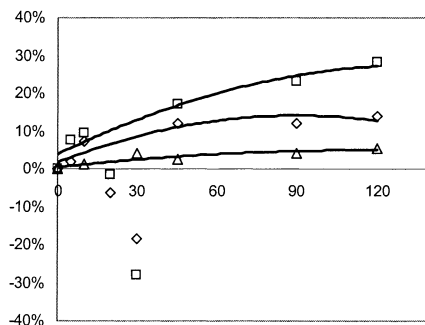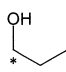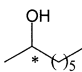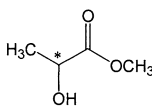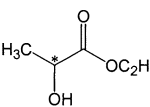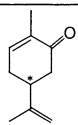

Figure 4. The long-term stability of the chiral coating of three sensors. The frequency deviation percentage Δf_t /Δf_0 over time (day). Δf_t, the amount of coating loss in terms of frequency deviation (Hz); Δf_0, the total coating amount measured in frequency shift (Hz) at Day 0.

Table 1. Chiral discrimination factor ($\overline{\alpha}_{R/S}$) of three QCM chiral sensors towards 5 pairs of enantiomers (Temp., 25.0°C, N$_2$ flowing rate, 200ml/min).

Devices		Analytes				
		2-butanol	2-octanol	Methyl lactate	Ethyl lactate	Carvone
		2.0μl[a]	0.5μl	2.0μl	1.0μl	1.0μl
CD1	Δf(Hz) (R/S)	-58/-54	-115/-103	-49/-44	-67/-60	-61/-56
CD2		-58/-53	-95/-86	-65/-58	-68/-61	-60/-55
CD3		-60/-54	-56/-51	-72/-64	-65/-58	-56/-52
CD1		46	152	157	108	1110
CD2	t(s)	47	168	165	111	1154
CD3		49	140	159	104	1065
GC[b]		1.081[c]	1.020[c]	1.119[e]	1.119[e]	1.02[d]
CD1	$\overline{\alpha}_{R/S}$	1.074	1.116	1.114	1.117	1.089
CD2		1.094	1.105	1.121	1.115	1.090
CD3		1.111	1.098	1.125	1.121	1.076

[a] sample injection volume; [b] reported optimal separation factors by GC.
[c] on 2,3,6-Tri-O-β-CD/OV-1701 column;[15b]
[d] on permethyl-O-(S)-2-hydroocypropyl-derivatized α-CD capillary GC[15a];
[e] on QCM coated with chiral amides by Bodenhöfer et al.[4]

In comparison with the reported GC separation factors towards 2-butanol, 2-octanol and carvone,[15] the three QCM sensors in this study exhibit superior chiral discriminatory ability,

in which the improvement of $\alpha_{R/S}$ is up to 9.5% by **CD1**. Although there has been no clear explanation thus far as to the actual mechanism behind the chiral discrimination process in GC, several factors such as operation temperature, substrate structure, mobile phase, etc. are known to affect enantioselectivity of chiral receptors to a certain extent.[16] In this study, the improved chiral discrimination ability could be the result of an ordered surface morphology in the monolayers. The permethylated βCD molecules self-assembled on the Au(111) surface afforded an ordered packing on the surface that would result in the increased number of binding sites accessible by chiral analytes. In particular, the interference from substrates and mobile phases would have been minimized in contrast to the situation of CSPs in GC.

Amenability to working under ambient temperature is another advantage of these chiral QCM sensors, and lower working temperature may also contribute to the improved chiral discriminative performances. While in GC, it is necessary for the columns to operate at elevated temperature to ensure optimal separation that usually result in lower separation factors.

In comparison with the chiral discriminatory results achieved on the chiral amides coated QCM sensors for methyl lactate and ethyl lactate,[4] the permethylated βCD deposited QCM sensors only achieve marginal improvement, about 0.5% in the case of methyl lactate. This could be attributed to the weak interaction presented between these guest molecules (methyl lactate, ethyl lactate, and 2-butanol) and permethylated βCD cavities due to the small size of the analyte molecule. Further studies on the influence of modified βCD cavity size on the complexation of these analytes in gas phase are currently undergoing in our laboratory on other modified βCD monolayers.

Chiral Sensor Recovery

For sensor recovery, since different sample sizes were involved, an easy comparison seems to be difficult here. Generally, all three QCM sensors can be recovered within a few minutes except in the case of carvone where the sensors experienced very slow recovery. The sensor recovery follows the sequence: $t_{2\text{-butanol}} \ll t_{2\text{-octanol}}$, $t_{\text{methyl lactate}} < t_{\text{ethyl lactate}}$, and t_{carvone} is the largest, where t is the time required for 95% recovery of frequency decrease in terms of the R-enantiomer of the analytes. In the case of carvone, t was measured only at 85% recovery of the sensor's resonant frequency change. Apparently the sensor recovery is strongly affected by the interactions between analyte molecules and βCD host molecules, which is closely related to

the molecular size of analytes due to the formation of inclusion complexes by βCD molecules. The bulky ring structure of carvone enhances the interactions with the interior wall of the permethylated βCD cavity, thus producing more stable transient inclusion complexes between carvone and permethylated βCD on the surface.[17]

Chiral Coating Stability

It is envisaged that the formation of Au-S bond between the cyclodextrinthiol derivatives and gold surface would render the enantioselective coating more environmentally durable. In addition, the length of the thiol spacer would exert an influence on the spatial arrangement and/ or surface concentration of the monolayer, which in turn will affect sensor properties. Accordingly, we examined the stability of chiral coatings having differing lengths of thiol spacers. The results are plotted in Figure 4. The deviation in the resonant frequency of **CD 1-3** (Δf_t) measured over time was compared with the resonant frequency of freshly coated QCMs (Δf_0 at Day 0). These coatings showed improved stability over time in N_2 stream, especially **CD3** with a longer spacer, which only displayed an increase of 9 Hz after 120 days corresponding only to a 5.4 % loss of the original surface coating. Data points with negative frequency deviation were recorded immediately after the chiral sensing measurement indicating that some guest molecules have remained inside the cavities of βCDs despite being purged with N_2 for prolonged periods.

Conclusion

In summary, we have demonstrated the applicability of self-assembled permethylated βCD monolayers as the enantioselective material for QCM chiral sensing. The resulting chiral sensors exhibit enhanced enantiomeric discriminatory ability and excellent long-term stability making it a potential candidate for real-time chiral sensing applications. Moreover, this approach provides a simplified model for a facile study of host-guest interactions: one theoretical plate instead of thousands in GC, room temperature instead of at elevated conditions of GC, and no interference from the substrate.

Support Structural Data.

(6^A-ω-mercapto-ethylureado-6^A-deoxy)heptakis(2,3-di-*O*-methyl)-6^B, 6^C, 6^D, 6^E, 6^F, 6^G-hexa-*O*-methyl-β-cyclodextrin (CD1) IR (cm^{-1}): 3396 (N-H str), 2931 (C-H str), 1668 (C=O

str, urea), 1040 (C-O-C str), ^{13}C-NMR (CDCl$_3$, 75 MHz) δ (ppm): 158.72 (-NH-$\underline{C}$O-NH-), 98.73 (C-1), 81.66 (C-2), 80.24 (C-3), 80.02 (C-4), 71.16 (C-6b), 70.83 (C-5), 67.73 (C-6a), 61.11 (H$_3$$\underline{C}$O-C3), 58.81 (H$_3$$\underline{C}$O-C6), 58.28 (H$_3$$\underline{C}$O-C2), 40.82 (-NH$\underline{C}H_2$-), 25.43 (-$\underline{C}H_2$-SH). ESI-MS: Calcd 1517.4, Found 1517.2. Elemental analysis: Calcd C 51.45%, H 7.70%, N 1.84%, S 2.11%; Found C 51.54%, H 7.51%, N 1.93%, S 1.95%.

(6^A-ω-mercapto-hexanureado-6^A-deoxy)heptakis(2,3-di-*O*-methyl)-6^B, 6^C, 6^D, 6^E, 6^F, 6^G-hexa-*O*-methyl-*β*-cyclodextrin (CD2) IR (cm^{-1}): 3399 (N-H str), 2930 (C-H str), 1657 (C=O str, urea), 1037 (C-O-C str). ^{13}C-NMR (CDCl$_3$, 75 MHz) δ (ppm): 159.00 (NH-$\underline{C}$O-NH), 98.76 (C-1), 81.66 (C-2), 81.32 (C-3), 80.22 (C-4), 71.40 (C-6b), 70.84 (C-5), 67.54 (C-6a), 61.18 (H$_3$$\underline{C}$O-C3), 58.90 (H$_3$$\underline{C}$O-C6), 58.47 (H$_3$$\underline{C}$O-C2), 41.22 (-NH$\underline{C}H_2$-), 38.67, 30.07, 28.99, 28.14 (-($\underline{C}$H$_2$)$_4$-), 26.44 (-$\underline{C}$H$_2$-SH). ESI-MS *m/z* Calcd 1573.5, Found 1596.5 for [M+Na]$^+$. Elemental analysis: Calcd C 52.67%, H 7.94%, N 1.78%, S 2.03%; Found C 52.71%, H 7.79%, N 1.76%, S 1.92%.

(6^A-ω-mercapto-undecanylureado-6^A-deoxy)heptakis(2,3-di-*O*-methyl)-6^B, 6^C, 6^D, 6^E, 6^F, 6^G-hexa-*O*-methyl-*β*-cyclodextrin (CD3) IR (cm^{-1}): 3396 (N-H str), 2928 (C-H str), 1659 (C=O str, urea), 1039 (C-O-C str). ^{13}C-NMR (CDCl$_3$, 75 MHz) δ (ppm): 159.02 (NH-$\underline{C}$O-NH), 98.70 (C-1), 81.64 (C-2), 81.35 (C-3), 80.26 (C-4), 71.85 (C-6b), 70.97 (C-5), 67.68 (C-6a), 61.14 (H$_3$$\underline{C}$O-C3), 58.83 (H$_3$$\underline{C}$O-C6), 58.36 (H$_3$$\underline{C}$O-C2), 41.27 (-NH$\underline{C}H_2$-), 40.36-26.80 (-($\underline{C}H_2$)$_9$-), 24.44 (-$\underline{C}H_2$-SH). ESI-MS *m/z* Calcd 1643.6, Found 1666.1 for [M+Na]$^+$. Elemental analysis: Calcd C 54.05%, H 8.22%, N 1.70%, S 1.95%; Found C 54.49%, H 7.82%, N 1.29%, S 1.70%.

Acknowledgements

[1] S. Ahuja, *Chiral Separation by Chromatograohy* Oxford University Press, Washington D.C., **2000**, pp7-14.

[2] M.T. Cygan, G.E. Collins, T.D. Dunbar, D.L. Allara, C.G. Gibbs, and C.D. Gutsche, Calixarene Monolayers as Quartz Crystal Microbalance Sensing Elements in Aqueous Solution, *Anal. Chem.* **1999**, 71, 142.

[3] J. Ide, T. Nakamoto and T. Moriizumi, Discrimination of aromatic optical isomers using quartz-resonator sensors, *Sens Actuators A* **1995**, 49, 73.

[4] K. Bodenhöfer; A, Hieriemann; J. Seemann; G. Gauglitz; B. Koppenhoefer; W. Göpel, Chiral discrimination in gas phase using different transducers: Thickness shear mode resonators and reflectometric interference spectroscopy, *Anal. Chem.* **1997**, 69, 3058.

[5] K. Bodenhöfer; A, Hieriemann; J. Seemann; G. Gauglitz; B. Koppenhoefer; W. Göpel, Chiral discrimination using piezoelectric and optical gas sensors, *Nature*, **1997**, 387, 577.

[6] S. Flink, F. C. J. M. van Veggel, D.N. Reinhoudt, Sensor functionalities in self-assembled monolayers, *Adv. Mater.* **2000**, 12, 1315.

[7] From our own measurements, a spin-coated 10 MHz QCM device with permethylated βCD, which resulted in 600Hz decrease of resonant frequency after drying in N_2, would display 60-100Hz frequency increases during a period of 45 days after the initial measurement.

[8] L. F. Zhang; Y. C. Wong; L. Chen; C. B. Ching, and S. C. Ng, A facile immobilization approach for perfunctionalised cyclodextrin onto silica via the staudinger reaction, *Tetra. Lett.,* **1999**, 40, 1815.

[9] M.T. Rojas, R. Königer, J.F. Stoddart, and A.E. Kaifer, Supported monolayers containing preformed binding sites. Synthesis and interfacial binding properties of a thiolated β-cyclodextrin derivative, *J. Am. Chem. Soc.* **1995**, 117, 336. (b) M. Weisser, G. Nelles, P. Wohlfart, G. Wenz, and S. Mittler-Neher, Immobilization kinetics of cyclodextrins at gold surface, *J. Phys. Chem.* **1996**, 100, 17893. (c) J.-Y. Lee and S.-M. Park, Electrochemistry of guest molecules in thiolated cyclodextrin self-assembled monolayers: Implication of size-selective sensors, *J. Phys. Chem. B* **1998**, 102, 9940.

[10] H.S. Ji, S. McNiven, K.H. Lee, T. Saito, K. Ikebukuro, I. Karube, Increasing the sensitivity of piezoelectric odour sensors based on molecularly imprinted polymers, *Biosens. Bioelec.* **2000**, 15, 403. (b) T. Nakamoto, A. Iguchi, T. Moriizumi, Vapor supply method in odor sensing system and analysis of transient sensor responses, *Sens. Actuators B*, **2000**, 71, 155.

[11] L. Van Vaeck, A. Adriaens, R. Gijbels, Static secondary ion mass spectrometry (S-SIMS) Part I: Methodology and structural interpretation, *Mass Spectrom. Rev.* **1999**, 18, 1.

[12] A.W. Czanderna and C. Lu, *Applications of Piezoelectric Quartz Crystal Microbalances* Elsevier, New York, **1984**, pp 145.

[13] S. Mitter-Neher, J. Spinke, M. Liley, G. Nelles, M. Weisser, R. Back, G. Wenz, W. Knoll, Spectroscopic and surface-analytical characterization of self-assembled layers on Au, *Biosens. Bioelec.* **1995**, 10, 903.

[14] J. Qian, R. Hentschke, W. Knoll, Superstructures of cyclodextrin derivatives on Au(111): A combined random planting-molecular dynamics approach, *Langmuir* **1997**, 13, 7092.

[15] D. W. Armstrong, W. Li, C. D. Chang, Polar-liquid, derivatized cyclodextrin stationary phases for the capillary gas chromatography separation of enantiomers, *Anal. Chem.* **1990**, 62, 914. (b) A. Berthod, W. Li, D. W. Armstrong, Multiple enantioselective retention mechanisms on derivatized cyclodextrin gas chromatography chiral stationary phase, *Anal. Chem.* **1992**, 64, 873.

[16] T. O'Brien, L. Crocker, R. Thompson, K. Thompson, P.H. Toma, D.A. Conlon, B. Feibush, C. Moeder, G. Bicker, and N. Grinberg, Mechanistic aspects of chiral discrimination on modified cellulose, *Anal. Chem.* **1997**, 69, 1999.

[17] K. B. Lipkowitz, G. Pearl, R. Coner, M. A. Peterson, Explanation of where and how enantioselective binding takes place on permethylated β-cycclodextrin, a chiral stationary phase used in gas chromatography, *J. Am. Chem. Soc.* **1997**, 119, 600.